Wavefront control for minimization of speckle coupling into a fiber injection unit based on the electric field conjugation algorithm

Jorge Llop Sayson, Dimitri Mawet, Garreth Ruane, Jacques-Robert Delorme, Daniel Echeverri, et al.

Jorge Llop Sayson, Dimitri Mawet, Garreth Ruane, Jacques-Robert Delorme, Daniel Echeverri, Nemanja Jovanovic, Nikita Klimovich, Yeyuan Xin, "Wavefront control for minimization of speckle coupling into a fiber injection unit based on the electric field conjugation algorithm," Proc. SPIE 10703, Adaptive Optics Systems VI, 1070372 (12 July 2018); doi: 10.1117/12.2313657

SPIE.

Event: SPIE Astronomical Telescopes + Instrumentation, 2018, Austin, Texas, United States

Wavefront control for minimization of speckle coupling into a fiber injection unit based on the electric field conjugation algorithm

Jorge Llop Sayson[a], Dimitri Mawet[a,b], Garreth Ruane[a], Jacques-Robert Delorme[a], Daniel Echeverri[a], Nemanja Jovanovic[a], Nikita Klimovich[a], and Yeyuan Xin[a]

[a]California Institute of Technology, 1200 E California Blvd., Pasadena, CA 91125
[b]Jet Propulsion Laboratory, , California Institute of Technology, 4800 Oak Grove Drive, Pasadena, CA 91109

ABSTRACT

A fiber injection unit situated in the focal plane behind a coronagraph feeding a high resolution spectrograph can be used to couple light from an exoplanet to obtain high resolution spectra with improved sensitivity. However, the signal-to-noise ratio of the planet signal is limited by the coupling of starlight into the single mode fiber. To minimize this coupling, we need to apply a control loop on the stellar wavefront at the input of the fiber. We present here a wavefront control algorithm based on the formalism of the Electric Field Conjugation (EFC) controller that accounts for the effect of the fiber. The control output is the overlap integral of the electric field with the fundamental mode of a single mode fiber. This overlap integral is estimated by sending probes to a deformable mirror. We present results from simulations, and laboratory results obtained at the Caltech Exoplanet Technology Lab's transmissive testbed. We show that our approach offers a significant improvement in starlight suppression through the fiber relative to a conventional EFC controller. This new approach improves the contrast of a high contrast instrument and could be used in future missions.

Keywords: High contrast imaging, Wavefront control, Wavefront sensing, Fiber injection unit, Electric Field Conjugation

1. INTRODUCTION

A great deal of effort has been invested into advancing high contrast imaging and spectroscopy technologies for exoplanet science. However, detecting biosignatures in faint exoplanets with direct imaging techniques still poses an immense challenge. The limitations on the possible telescope's primary mirror sizes, and segmented configurations, combined with the presence of aberrations throughout the optical system, limit the detectability of biosignatures due to the presence of unwanted stray light from the host star. Furthermore, the wavefront stability requirements for detecting and characterizing Earth-like exoplanets at a contrast of 10^{-10} with missions like LUVOIR[1] and HabEx,[2] will likely be of the order of a few pico-meters, at the limits of what is possible on current high contrast testbeds.

High Dispersion Coronagraphy[3,4] is a novel concept that aims at combining high contrast imaging with high dispersion spectroscopy to characterize exoplanets. This concept includes a fiber injection unit (FIU) placed downstream of a coronagraphic mask. The purpose of the FIU is to recover the planet signal by coupling its light through a single mode fiber (SMF). However, in the process of coupling planet light to the SMF, residual star light, couples into the fiber as well. The SNR of the planet light is limited by the photon noise from the coupled star light which is still relatively bright at the location of the planet. Indeed, the motivation of using a single mode fiber is to exploit its mode selectivity, yet diffracted starlight signal can still get coupled into the fiber. Controlling the electric field that couples into the fiber is critical to reduce photon noise so that the faint planet signal can be analyzed.

Wavefront control techniques aim at eliminating the speckles using Adaptive Optics (AO) systems. A deformable mirror (DM) placed at a pupil plane aims at modifying the incoming wavefront to create a dark, speckle-free region in the image plane. For this, several approaches have been implemented successfully in laboratory demonstrations,[5] a notable example is the electric field conjugation, or EFC,[6] algorithm, which is the

Adaptive Optics Systems VI, edited by Laird M. Close, Laura Schreiber, Dirk Schmidt, Proc. of SPIE Vol. 10703, 1070372 · © 2018 SPIE
CCC code: 0277-786X/18/$18 · doi: 10.1117/12.2313657

baseline wavefront control algorithm for the WFIRST Coronagraph Instrument (CGI). With EFC, the shape of the DM, characterized by a NxN actuator heights, is solved giving the least squares minimum of the electric field.

We introduce here a new algorithm based on EFC formalism to control the wavefront in order to minimize the speckles coupling into the a SMF. We present the modified formalism from EFC that accounts for the modal selectivity of the SMF, we show results from simulations, and laboratory results.

2. ELECTRIC FIELD SENSING

EFC aims at suppressing iteratively the electric field in a region of the image plane, hence, EFC needs an estimate of the electric field. In the case of a SMF, the measured intensity in the output of the fiber is the overlap integral of the electric field at the input of the fiber multiplied by the fundamental mode of the fiber:

$$I = \left| \int_{fxel} E_{im} \Psi_{SMF} dx \right|^2 \tag{1}$$

Where E_{im} is the electric field in the image plane, and Ψ_{SMF} is the fiber mode shape. Therefore, this results in the inability to measure the true field in the image plane. However, even if the electric field cannot be estimated if we close the loop on a SMF, the control algorithm presented here relies on the sensing of the overlap integral complex number, i.e. the overlap integral of both the real and imaginary parts of the electric field.

The procedure for sensing the overlap integral is based on the method presented by Give'On et al. 2009,[6] as presented by Groff et al. 2015.[5] This method is often called Pair-wise probing.

The electric field in the image plane is:

$$E_{im} = \mathcal{C}(A\ e^{\alpha+i\beta} e^{i\phi}) \tag{2}$$

Where A is the pupil field, α, and β, are the amplitude and phase aberrations, ϕ is the shape of the DM, and $\mathcal{C}(\cdot)$ is the coronagraph operator. Expanding assuming small aberrations:

$$E_{im} \approx \mathcal{C}(A\ e^{\alpha+i\beta}) + i\mathcal{C}(\phi) \tag{3}$$

$$= E_{Sp} + Gu \tag{4}$$

Where E_{Sp} is the speckle field we want to retrieve, G is the control effect matrix, and u contains the amplitude change on the DM. The intensity measured at the output of a fiber:

$$I = \left| \int_{fxel} (E_{Sp} + Gu) \Psi_{SMF} dx \right|^2 \tag{5}$$

It can be shown that:

$$I = \left| \int_{fxel} \Psi_{SMF} E_{Sp} dx + \int_{fxel} \Psi_{SMF} G u dx \right|^2 \tag{6}$$

$$= \left| \int_{fxel} \Psi_{SMF} E_{Sp} dx \right|^2 + \left| \int_{fxel} \Psi_{SMF} G u dx \right|^2 + 2Re\{ \int_{fxel} \Psi_{SMF} E_{Sp} dx \cdot \int_{fxel} \Psi_{SMF} G u dx \} \tag{7}$$

For a pair of probes, $\pm Gu$, the difference between intensities of the positive and negative probe images:

$$\Delta I = 4Re\{\int_{fxel} \Psi_{SMF} E_{Sp} dx \cdot \int_{fxel} \Psi_{SMF} G u dx\} \tag{8}$$

$$\Delta I = 4(Re\{\int_{fxel} \Psi_{SMF} E_{Sp} dx\} Re\{\int_{fxel} \Psi_{SMF} G u dx\} + Im\{\int_{fxel} \Psi_{SMF} E_{Sp} dx\} Im\{\int_{fxel} \Psi_{SMF} G u dx\}) \tag{9}$$

$$\Delta I = 4 \int_{fxel} \Psi_{SMF} Re\{E_{Sp}\} dx \int_{fxel} \Psi_{SMF} Re\{Gu\} dx + 4 \int_{fxel} \Psi_{SMF} Im\{E_{Sp}\} dx \int_{fxel} \Psi_{SMF} Im\{Gu\} dx \tag{10}$$

This is for a measurement of a pair of probes. For n different pairs of probes in matrix form:

$$\begin{bmatrix} \Delta I_1 \\ \vdots \\ \Delta I_n \end{bmatrix} = 4 \begin{bmatrix} \int_{fxel} \Psi_{SMF} Re\{Gu_1\} dx & \int_{fxel} \Psi_{SMF} Im\{Gu_1\} dx \\ \vdots & \vdots \\ \int_{fxel} \Psi_{SMF} Re\{Gu_n\} dx & \int_{fxel} \Psi_{SMF} Im\{Gu_n\} dx \end{bmatrix} \begin{bmatrix} \int_{fxel} \Psi_{SMF} Re\{E_{Sp}\} dx \\ \int_{fxel} \Psi_{SMF} Im\{E_{Sp}\} dx \end{bmatrix} \tag{11}$$

Or:

$$z = H\ x \tag{12}$$

Taking the pseudo-inverse of the observation matrix H, we find an estimate of the electric field:

$$\hat{x} = H^{-\dagger}\ z \tag{13}$$

Where, $\hat{x}$ is the estimate of the complex number of the overlap integral that will be used in the wavefront control. Therefore, although we are unable to estimate the actual electric field that falls on the tip of the SMF, we estimate the overlap integral, i.e. the light going through the SMF, which is the variable we are interested in for the control algorithm. This estimate is computed at each control iteration.

3. EFC WITH A SINGLE MODE FIBER

Once the overlap integral of the electric field in the image plane is estimated, the usual EFC algorithm can be used. We use the algorithm presented in Give'On et al.[6] Assuming small aberrations, and small effects of the DM on the image plane, as previously done in Sec. 2, the electric field at the image plane can be written as:

$$E_{im} = E_{Sp} + Gu \tag{14}$$

EFC seeks to minimize the output of the fiber. As discussed in Sec. 2, the control parameter the algorithm has access to is the complex overlap integral number, $\hat{x}$ in Eq. 13 . Therefore, the algorithm computes the DM shape that minimizes the overlap integral:

$$u = -G^{-\dagger} \hat{x} \tag{15}$$

$$= -G^{-\dagger} \begin{bmatrix} \int_{fxel} \Psi_{SMF} Re\{E_{Sp}\} dx \\ \int_{fxel} \Psi_{SMF} Im\{E_{Sp}\} dx \end{bmatrix} \tag{16}$$

The control effect matrix G takes a different form for this algorithm. In regular EFC, G accounts for the effect of each actuator on every element of the dark hole. In the case of a SMF, G accounts for the effect of each actuator on the overlap integral. Hence, G is computed in a similar manner to how is computed in regular EFC. Using a model of the optical system, each actuator is poked and its effect on the overlap integral of the electric field is registered in G.

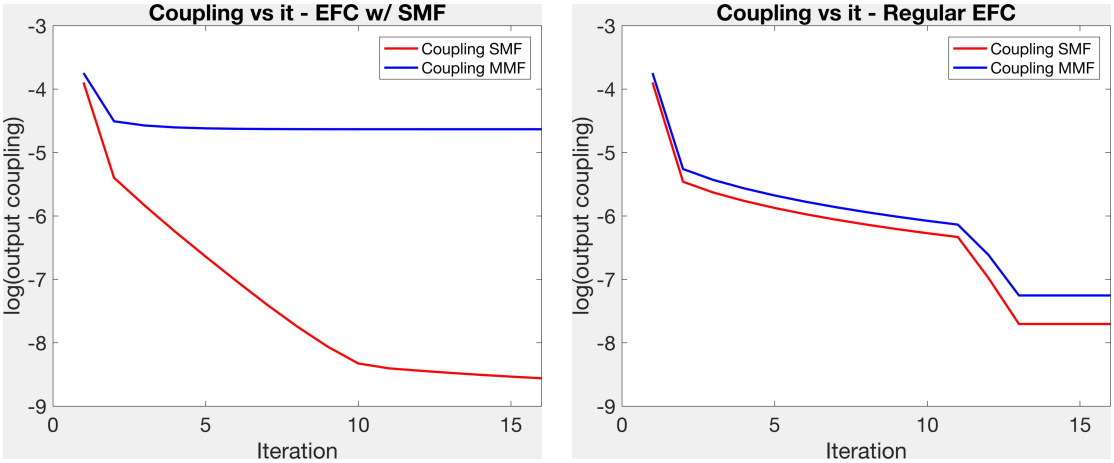

Figure 1. We perform EFC with the new algorithm (left), and regular EFC (right), and calculate the contrast achieved through a single mode fiber (SMF, red), and a multimode fiber (MMF, blue), which would be the equivalent of having pixels. Simulation at 10% broadband light

The computation of the shape of the DM, u, is done iteratively, until the null through the SMF converges to a final raw contrast solution.

4. SIMULATION RESULTS

In order to validate the control algorithm presented above, we performed preparatory simulations in an end-to-end testbed simulation of the High Contrast Spectroscopy for Segmented Telescopes Testbed (HCST) in the Exoplanet Technology Laboratory (ET Lab) at Caltech. This model is based on a MATLAB code that uses the PROPER[7] library to perform realistic propagations for coronagraph and adaptive optics systems.

For monochromatic light at 650 nm we obtain virtually complete suppression of the coupling of the speckles through the fiber; the DM at the pupil plane has full control authority over the coupling of any monochromatic speckle through a single mode fiber placed within the control area on the image plane.

We simulated the algorithm performance at 10% bandwidth light, centered at 650 nm wavelength, and compared it to the performance on the same setup, and speckle field, for regular EFC, see Fig. 1. In both simulations we compute the intensity read at the output of a SMF, and the output of a multi mode fiber (MMF), which is equivalent to the intensity read from conventional pixels. This assumes all the light in the area of the MMF couples into the fiber, i.e. no mode overlap considered here. In order to compare both outputs, we calculate the MMF entrance diameter by making the throughput equivalent to that of our SMF when centered to the non-coronagraphic PSF. The performance of the new algorithm is consistently better for different error maps on the optical setup than regular EFC in terms of minimizing the speckle coupling into the fiber.

As discussed in Sec. 3, the new algorithm does not try to eliminate the electric field at the fiber position, instead, it minimizes the overlap integral of the speckles with the fundamental mode of the SMF. This important difference between the new algorithm presented here and regular EFC can be seen in the result of running both and comparing the result at the image plane, as can be seen in Fig. 2. Although more light falls on the region of the fiber for the new algorithm result with respect to the regular EFC result, there is less light coupling into the SMF, which is what we are interested in. The cost function is less restrictive, and the algorithm is not required to move the same amount of light from the region of the fiber, therefore the DM strokes are significantly smaller, as it can be seen in Fig. 3. Two main factors help explain this fact: (1) the modal selectivity of the SMF helps relieve the work of the DM, and (2) the fact that regular EFC works with several resolution elements to effectively suppress the stray light in the region of the fiber makes its cost function more restrictive.

In Fig. 4, and Fig. 5, we zoom into the region of the fiber, and compare the intensity and phase, respectively, in the region, for both a regular EFC run and a run of the new algorithm. As it can be seen in Fig. 4, regular

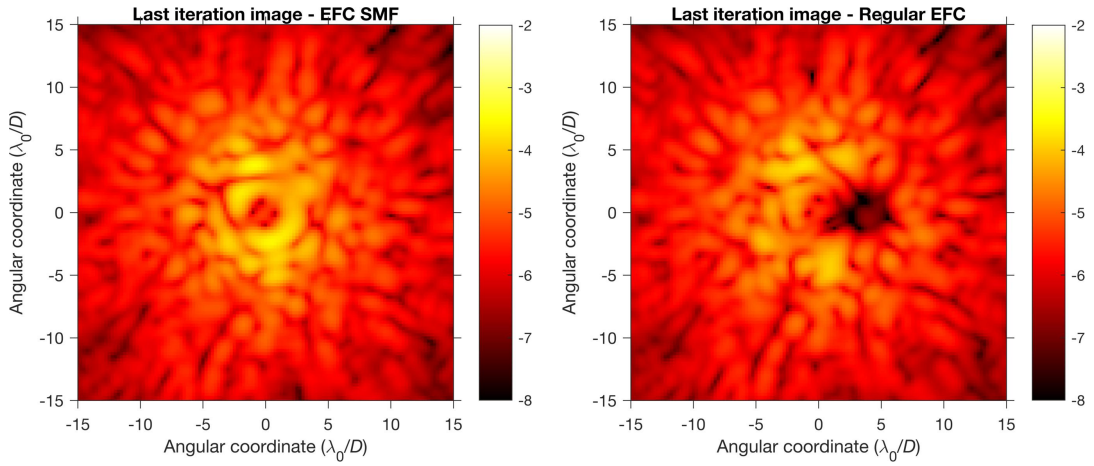

Figure 2. The results from the new algorithm (*left*) have a smaller effect on the final image w.r.t. the results from running regular EFC (*right*), however, the overlap integral is better nulled in the former case. Indeed, the new algorithm seeks to minimize the overlap integral of the electric field, and not the actual electric field as it is the case for regular EFC.

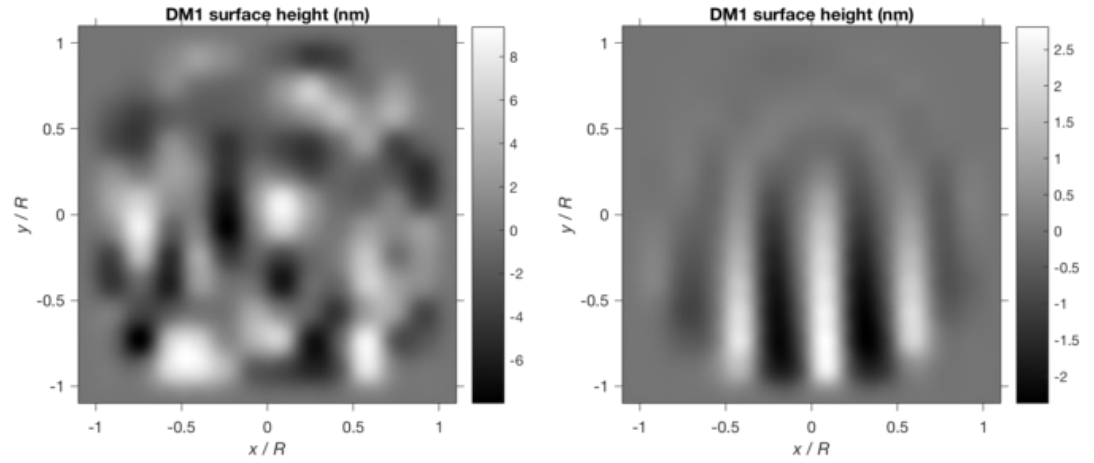

Figure 3. The final DM solution for the regular EFC run (*left*), has higher strokes on the DM actuators with respect to the solution of the DM for the new algorithm (*right*). This is explained by the fact that the new algorithm has a less restraining cost function.

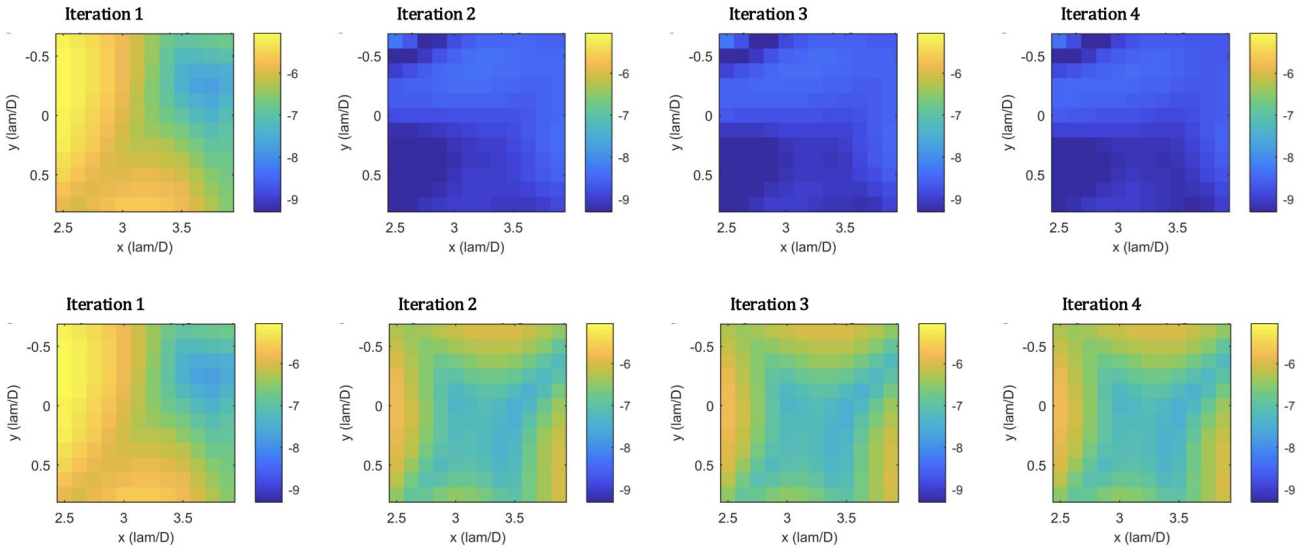

Figure 4. Zooming into the region of the fiber, the first 5 iterations on a regular EFC run (*top*) show how EFC tries to suppress the intensity over the region. However, the new algorithm works on create a phase pattern that suppresses the overlap integral.

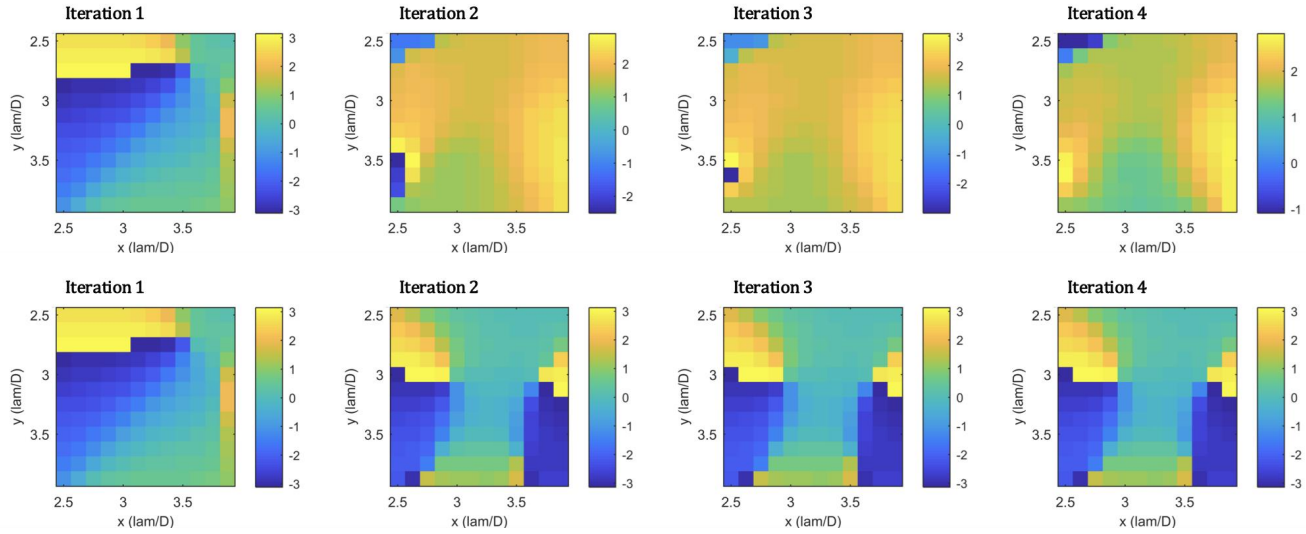

Figure 5. Zooming into the region of the fiber, the first 5 iterations on a regular EFC run (*top*) show how the phase over the region of the fiber does not find a pattern since EFC works on suppressing the entire electric filed on the region. However, for the new algorithm (*bottom*) the phase builds a vortex pattern on the region of the fiber.

EFC tries to suppress the electric field, thus the intensity, however, the phase doesn't seem to find any pattern (see Fig. 5). On the other hand, for the new algorithm, the intensity in not suppressed, but the phase forms vortex patterns over the fiber position.

5. LABORATORY TESTS

To validate the algorithm we performed laboratory tests at HCST, in the ET Lab at Caltech.

5.1 Laboratory Setup

The setup used for these tests was the HCST-T,[4] an optical testbed consisting of transmissive optics, a DM, a coronagraph system, and a FIU (See Fig. 6). The optics used are off the shelf transmissive lenses; the DM, a Boston MEMS multi-DM, a 12×12 actuator DM; the coronagraph, a vortex charge 8. At the FIU, a dichroic lets the majority of the light go through to the fiber optics, and reflect light to the tracking camera. The use of the camera is for positioning of the fiber and alignment of the coronagraph mask.

5.2 Laboratory Results

Fig. 7, shows a laboratory demonstration of the new algorithm, in which a suppression of a factor of ∼3 is achieved through the SMF. Although this suppression level is not as great as expected from simulations, we have some suppositions as to why the lab performance may be limited. Despite the modest improvement in star light suppression this is the first demonstration of the control of the electric field through an optical fiber using the EFC formalism.

Problems typically encountered in EFC may be hindering our performance. One of the biggest challenges in EFC is having a reliable model of the physical system, to both estimate the electric field, in our case the overlap integral, and to built the Jacobian of the system. The quality of the optics in our setup, plus the uncertainties in the alignment, are hard to model. Another problem we are probably facing is the stability of the bench. The setup is in open air, so air turbulence makes the PSF move around the image plane. We have measured high frequency oscillations with an amplitude of 20% of λ/D approximately. Furthermore, we have measured a lower frequency drift, in the order of minutes, of the PSF of the order of 1 λ/D. Finally, given the quality of the optics and the fact they are transmissive lenses, we may not be working in a fully linear regime; a starting point of 3×10^{-3} raw contrast may be making EFC hard to work.

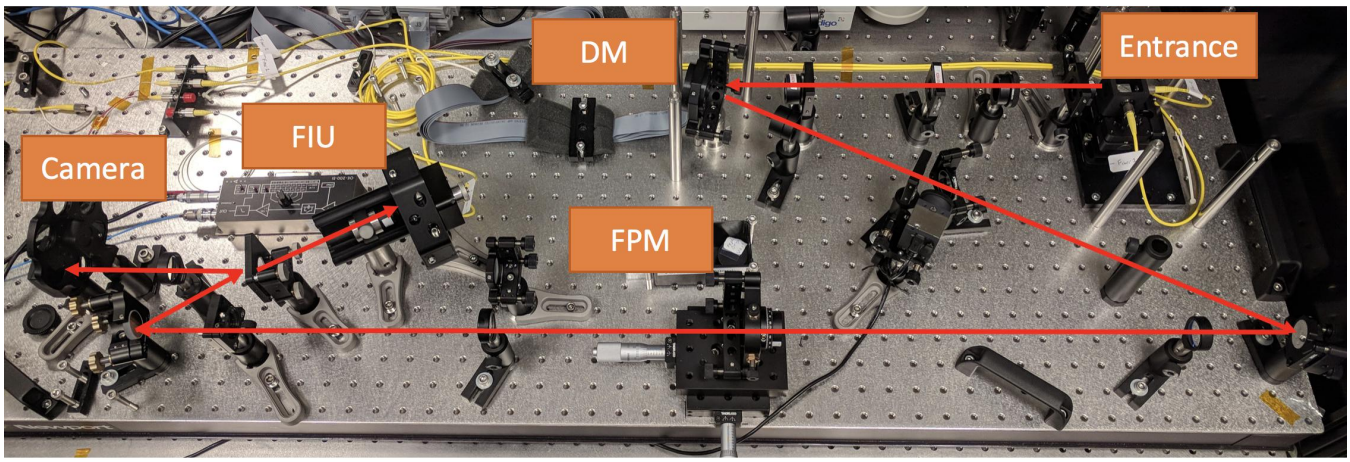

Figure 6. HCST-T consists on a AO system with a Boston MicroMachines Corporation (BMC) MEMS multi-DM 12×12 actuators DM, a coronagraph with a vortex coronagraph, and a FIU.

6. FUTURE WORK AND CONCLUSIONS

After having demonstrated this new algorithm at HCST-T, we plan to move the experiment to HCST-R.[8] Equipped with custom reflective optics and a BMC kilo-DM, HCST-R has an enormous potential for exploring high contrast technologies. Ruane et al.[8] in these proceedings demonstrated a raw contrast of 5×10^{-8} using a simple Speckle Nulling technique, our plan is to include a FIU at the image plane of HCST-R and achieve very high contrast through the SMF.

A Kalman Filter was implemented for Speckle Nulling by Xin et al. in these proceedings,[9] in which the control history, and previous measurements, were used to achieve a more stable null through the SMF, and an overall better raw contrast, in the order of 10% improvement. A Kalman Filter Estimator for EFC was proven

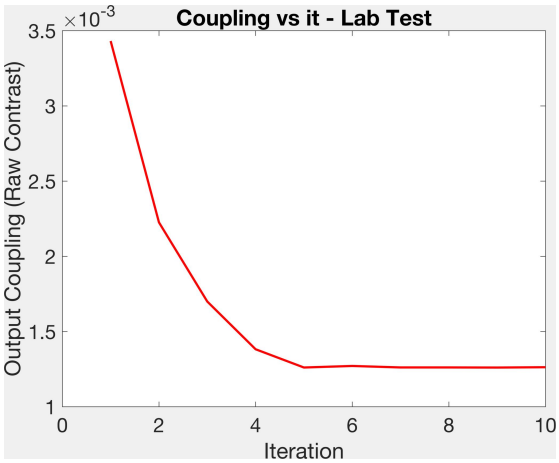

Figure 7. We achieve speckle suppression through the SMF in the laboratory, with a factor of ∼2-3 consistently in our experiments.

by Groff, et al. 2013,[10] for a faster suppression of the electric field of the starlight in an EFC dark hole. This technique can be directly applied for the case of EFC for a FIU, we plan to demonstrate this at the ET Lab. Predictive control is particularly important in the presence of atmospheric turbulence; a Kalman Filter approach, which can account for the nature of the speckle evolution in the image plane, is a very promising technique.

We also plan on demonstrating this technique on sky. The Keck Planet Imager and Characterizer[11] (KPIC) is a concept developed for the Keck Observatory consisting of a module with a dedicated channel for a FIU. As well as its unique science capabilities, KPIC is also intended as a path to mature key technologies, such as HDC, for future space based telescopes and large ground-based telescopes such as the Thirty Meter Telescope. KPIC is a perfect instrument to test this algorithm with real data in real time.

The wavefront control presented here is designed to take advantage of the SMF, thus is perfectly suited for an HDC system. The promising results obtained from simulations, and the lessons learned from applying EFC in the laboratory, will help us achieve the levels of contrast we are aiming for. Achieving this in practice on future telescopes will enable the detection of spectral signatures associated with individual molecules and potential signs of life.

REFERENCES

[1] Bolcar, M. R., Aloezos, S., Bly, V. T., Collins, C., Crooke, J., Dressing, C. D., Fantano, L., Feinberg, L. D., France, K., Gochar, G., Gong, Q., Hylan, J. E., Jones, A., Linares, I., Postman, M., Pueyo, L., Roberge, A., Sacks, L., Tompkins, S., and West, G., "The Large UV/Optical/Infrared Surveyor (LUVOIR): Decadal Mission concept design update," in [*Society of Photo-Optical Instrumentation Engineers (SPIE) Conference Series*], *Society of Photo-Optical Instrumentation Engineers (SPIE) Conference Series* **10398**, 1039809 (Sept. 2017).

[2] Mennesson, B., Gaudi, S., Seager, S., Cahoy, K., Domagal-Goldman, S., Feinberg, L., Guyon, O., Kasdin, J., Marois, C., Mawet, D., Tamura, M., Mouillet, D., Prusti, T., Quirrenbach, A., Robinson, T., Rogers, L., Scowen, P., Somerville, R., Stapelfeldt, K., Stern, D., Still, M., Turnbull, M., Booth, J., Kiessling, A., Kuan, G., and Warfield, K., "The Habitable Exoplanet (HabEx) Imaging Mission: preliminary science drivers and technical requirements," in [*Space Telescopes and Instrumentation 2016: Optical, Infrared, and Millimeter Wave*], **9904**, 99040L (July 2016).

[3] Wang, J., Mawet, D., Ruane, G., Hu, R., and Benneke, B., "Observing Exoplanets with High Dispersion Coronagraphy. I. The Scientific Potential of Current and Next-generation Large Ground and Space Telescopes," **153**, 183 (Apr. 2017).

[4] Mawet, D., Ruane, G., Xuan, W., Echeverri, D., Klimovich, N., Randolph, M., Fucik, J., Wallace, J. K., Wang, J., Vasisht, G., Dekany, R., Mennesson, B., Choquet, E., Delorme, J.-R., and Serabyn, E., "Observing Exoplanets with High-dispersion Coronagraphy. II. Demonstration of an Active Single-mode Fiber Injection Unit," **838**, 92 (Apr. 2017).

[5] Groff, T. D., Eldorado Riggs, A. J., Kern, B., and Jeremy Kasdin, N., "Methods and limitations of focal plane sensing, estimation, and control in high-contrast imaging," *Journal of Astronomical Telescopes, Instruments, and Systems* **2**, 011009 (Jan. 2016).

[6] Give'On, A., "A unified formailism for high contrast imaging correction algorithms," in [*Techniques and Instrumentation for Detection of Exoplanets IV*], **7440**, 74400D (Aug. 2009).

[7] Krist, J. E., "Proper: an optical propagation library for idl," (2007).

[8] Ruane, G., Mawet, D., Delorme, J., Jovanovic, N., Echeverri, D., Llop Sayson, J., Zhang, R., Eldorado Riggs, A., Shaklan, S., Serabyn, E., and J.K., W., "Laboratory testing of coronagraphs for future space telescopes on the Caltech high contrast spectroscopy testbed for segmented telescopes (HCST)," (2018).

[9] Xin, Y., Klimovich, N., Mawet, D., Ruane, G., Delorme, J., Jovanovic, N., and Llop Sayson, J., "Demonstration of a Speckle Nulling Algorithm and Kalman Filter Estimator with a Fiber Injection Unit for Observing Exoplanets with High-dispersion Coronagraphy," (2018).

[10] Groff, T. D. and Jeremy Kasdin, N., "Kalman filtering techniques for focal plane electric field estimation," *Journal of the Optical Society of America A* **30**, 128 (Jan. 2013).

[11] D. Mawet, J. R. Delorme, N. J. J. K. W. R. D. B. P. L. W. M. F. S. L. G. R. J. W. N. K. Y. X., "A fiber injection unit for the keck planet imager and characterizer," (2017).